

## Nonequilibrium Dynamics in a Quasi-Two-Dimensional Electron Plasma after Ultrafast Intersubband Excitation

Stephan Lutgen, Robert A. Kaindl, Michael Woerner, and Thomas Elsaesser  
*Max-Born-Institut für Nichtlineare Optik und Kurzzeitspektroskopie, D-12489 Berlin, Germany*

Andreas Hase and Harald Künzel  
*Heinrich-Hertz-Institut für Nachrichtentechnik Berlin GmbH, D-10587 Berlin, Germany*

Mario Gulia  
*INFN-Dipartimento di Fisica, Università di Modena, I-4100 Modena, Italy*

Duilio Meglio and Paolo Lugli  
*INFN-Dipartimento di Ingegneria Elettronica, Università di Roma Tor Vergata, I-00133 Roma, Italy*  
 (Received 31 May 1996)

The dynamics of electrons in GaInAs/AlInAs quantum wells is studied after excitation from the  $n = 1$  to the  $n = 2$  conduction subband. Femtosecond pump-probe experiments demonstrate for the first time athermal distributions of  $n = 1$  electrons on a surprisingly long time scale of 2 ps. Thermalization involves intersubband scattering of excited electrons via optical phonon emission with a time constant of 1 ps and intrasubband Coulomb and phonon scattering. Ensemble Monte Carlo simulations show that the slow electron equilibration results from Pauli blocking and screening of carrier-carrier scattering. [S0031-9007(96)01482-2]

PACS numbers: 78.47.+p, 42.65.Re, 73.20.Dx

The fundamental nonequilibrium dynamics of carriers in semiconductors occurs on ultrafast time scales and is governed by the interaction between different elementary excitations of the carriers and the lattice. Optical spectroscopy with femtosecond time resolution allows the generation of well-defined distributions of nonequilibrium carriers and provides direct insight into the subsequent thermalization processes, i.e., the relaxation towards a quasiequilibrium (hot Fermi) distribution by carrier-carrier and carrier-phonon scattering [1–3]. In most experiments, electron-hole plasmas have been generated by excitation in the interband continuum and transient carrier distributions were derived from time-resolved measurements of nonlinear absorption or luminescence.

In quasi-two-dimensional semiconductors, the quantization of electron and hole states leads to a sequence of valence and conduction subbands and a new type of optical excitation, the intersubband (IS) transitions between consecutive bands. Because of the more or less parallel dispersion of such bands in  $k$ -space (energy versus in-plane  $k$ -vector), intersubband excitation of electrons leads to a different initial distribution of nonequilibrium carriers and a fundamentally different scenario of electron relaxation. This involves backscattering from higher to lower subbands, i.e., IS scattering, and electron thermalization in the lowest subband by intraband scattering. These processes are still not completely understood: First, different time-resolved optical experiments on intersubband scattering of electrons have provided quite contradictory information. For an energy separation of the subbands larger than the energy of a longitudinal optical (LO) phonon, re-

laxation times between about 200 fs and 10 ps have been claimed [4–7], whereas theoretical calculations suggest IS relaxation by LO phonon emission with time constants of about 1 ps [7–9]. Second, electron thermalization after intersubband excitation has not been explored until now and—thus—the dynamics and the mechanisms of equilibration are not known. An exact determination of the characteristic times of such processes is of crucial importance in view of the recent demonstration of infrared lasing action in semiconductor superlattices [10].

In this Letter, we report on a femtosecond study of electron relaxation after intersubband excitation in  $n$ -type modulation-doped GaInAs/AlInAs quantum wells (QWs). Because of the large barrier height of approximately 0.5 eV in this material system, both the ( $n = 1$ ) and ( $n = 2$ ) conduction subbands are strongly confined to the QWs. In contrast to most available experiments, we are able to study a single-component plasma by monitoring exclusively the electron dynamics. Femtosecond pulses in the midinfrared serve for a selective excitation of electrons from the ( $n = 1$ ) to the ( $n = 2$ ) subband. The time evolution of the transient carrier distributions is monitored directly by probing changes of the interband absorption with femtosecond pulses in the near infrared. This allows a separate observation of different relaxation stages. An IS scattering time of 1 ps is directly measured. We demonstrate for the first time that the transient distributions of ( $n = 1$ ) electrons occurring after IS excitation show a distinct athermal character and thermalize on a time scale of about 2 ps. Ensemble Monte Carlo (EMC) simulations of both the intersubband and intrasubband dynamics are

in quantitative agreement with the experiments and give evidence that the thermalization process is controlled by the balance between phonon and Coulomb scatterings.

In our experiments, we studied an  $n$ -type modulation-doped multiple quantum well structure which was grown by molecular beam epitaxy on an InP substrate. The sample consists of 50 Ga<sub>0.47</sub>In<sub>0.53</sub>As QWs of 8 nm width separated by 14 nm Al<sub>0.48</sub>In<sub>0.52</sub>As barriers. Si  $\delta$  doping in the center of the barriers prevents impurity scattering of QW carriers ( $n = 5 \times 10^{11} \text{ cm}^{-2}$ ). The femtosecond experiments performed at a lattice temperature of  $T_L = 8 \text{ K}$  are based on a pump-probe scheme shown in the inset of Fig. 1. Electrons are excited from the ( $n = 1$ ) to the ( $n = 2$ ) subband by bandwidth limited 130 fs midinfrared pulses which are resonant to the IS transition at  $\Delta E_{1,2} = 200 \text{ meV}$  (wavelength  $\lambda = 6.2 \mu\text{m}$ ). The transient electron distributions in both the ( $n = 1$ ) and ( $n = 2$ ) subband are monitored with 100 fs probe pulses (bandwidth 13 meV) via changes of the ( $n = 2$ ) and ( $n = 1$ ) valence to conduction band absorption in the near infrared. Pump and probe pulses are derived from a regeneratively amplified Ti:sapphire laser by parametric generation and difference frequency mixing [11] and spectral selection from a femtosecond white-light continuum, respectively. To achieve excitation of the IS dipole moment oriented perpendicular to the QW layer, the sample was put under Brewster angle in the pump beam of in-plane polarization. From the incident intensity, the sample transmission and the spot size on the sample we estimate an excitation density of 10% to 20% of the total electron concentration.

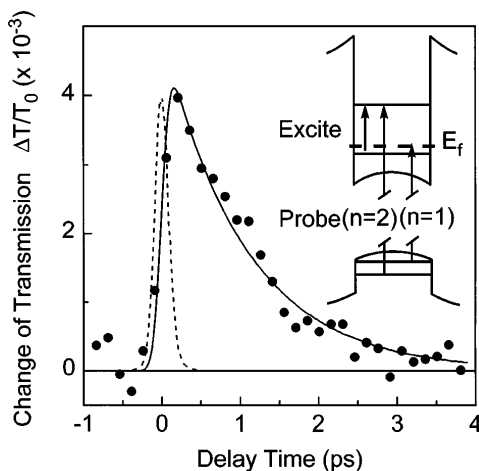


FIG. 1. Time-resolved transmission change of the ( $n = 2$ ) interband transition after excitation of  $n = 1$  electrons to the  $n = 2$  subband. The change of transmission  $\Delta T/T_0 = (T - T_0)/T_0$  (solid circles) is plotted vs the delay time between midinfrared excitation pulses ( $E_{\text{ex}} = 0.2 \text{ eV}$ ) and probe pulses at  $E_{\text{pr}} = 1.141 \text{ eV}$  ( $T, T_0$ : transmission with and without excitation). The Monte Carlo simulation gives a decay time of 1 ps (solid line). Dashed line: Cross correlation of pump and probe pulses. Inset: Pump-probe scheme of the experiments.

The experiments were simulated by an EMC approach described in its general lines in Refs. [12,13]. Intersubband and intrasubband electron-electron scatterings, Pauli exclusion principle, and nonequilibrium phonons are taken into account. The specific properties of the phonon modes in the GaInAs/AlInAs QWs were considered within the dielectric continuum model [8,9]. Intersubband excitation was simulated by promoting about 15% of the electrons from the ( $n = 1$ ) to the ( $n = 2$ ) subband by a 130 fs pulse that was resonant to the IS transition between the ( $n = 1$ ) and ( $n = 2$ ) conduction subbands of parallel in-plane  $k$ -dispersion. For comparison with the measured absorption changes, the difference between the transient and the initial electron distribution in each subband was multiplied with the steplike absorption coefficient of the respective valence to conduction band transition and convoluted with the temporal and spectral envelope of the 100 fs probe pulses (bandwidth 13 meV).

In Fig. 1, we present time-resolved data (symbols) taken at the onset of the ( $n = 2$ ) absorption in the range  $1.130 < E_{\text{pr}} < 1.150 \text{ eV}$  ( $E_{\text{pr}}$ : photon energy of the probe). The change of transmission  $\Delta T/T_0 = (T - T_0)/T_0$  is plotted versus delay time between the midinfrared pump pulses and the probe pulses ( $T_0, T$ : transmission of the sample before and after excitation). We observe a transient increase of transmission, i.e., a bleaching, which rises within the time resolution of the experiment and decays with a time constant  $\tau_{\text{IS}} = 1 \text{ ps}$ . The bleaching is caused by the transient electron population of the ( $n = 2$ ) conduction band, leading to a blocking of the corresponding interband transitions. The ( $n = 2$ ) population decays by intersubband scattering back to high-lying ( $n = 1$ ) states with  $\tau_{\text{IS}}$ . This decay is very well reproduced by the EMC simulation (solid line), indicating that the depopulation of the ( $n = 2$ ) subband for a subband spacing much higher than the energy of optical phonons is due to the emission of confined and interface phonons via the polar interaction [14].

To gain insight into the dynamics of the ( $n = 1$ ) electrons, transient absorption spectra were recorded in the range of the stationary ( $n = 1$ ) absorption edge around  $E_{\text{pr}} = 0.913 \text{ eV}$  (determined by the band gap of the QWs) and by the steady state electron distribution which populates the bottom of the ( $n = 1$ ) subband and blocks the corresponding interband transitions. In Fig. 2, we present spectra for various delay times after IS excitation (solid circles). At 0.2 ps [Fig. 2(a)], we observe a decrease of transmission in the range of the initially populated electron states which is due to depletion by the excitation pulse. At later times [Figs. 2(b)–2(e)], the amplitude of this signal rises and—in addition—a delayed bleaching occurs at higher photon energies. For comparison, data taken at delay times longer than 2 ps [cf.  $t_D = 11 \text{ ps}$ , open squares in Fig. 2(b)] exhibit a transmission decrease below and a bleaching above the Fermi edge which are of similar amplitude. Eventually,

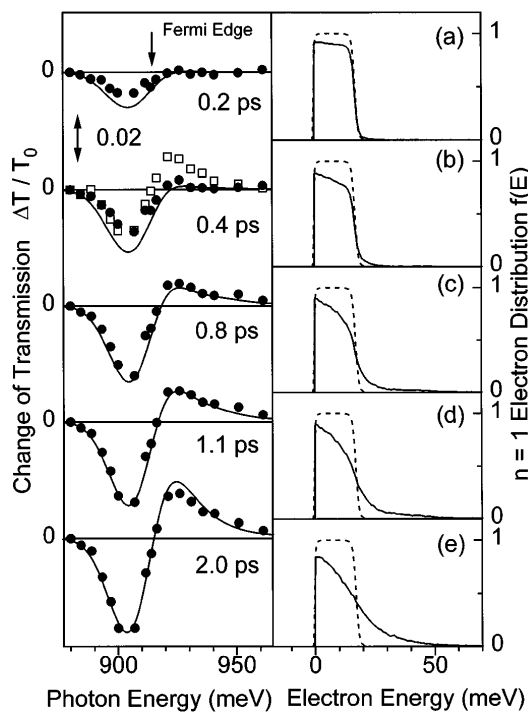


FIG. 2. Left-hand side: Transient spectra of the  $n$ -type modulation-doped GaInAs/AlInAs MQW structure in the spectral range of the  $(n = 1)$  interband transition after femtosecond intersubband excitation. The transmission change  $\Delta T/T_0$  is plotted as a function of the photon energy of the probe pulses for delay times of (a) 0.2, (b) 0.4, (c) 0.8, (d) 1.1, and (e) 2 ps (circles), as well as (b) 11 ps (squares) for comparison. The bandwidth of the probe pulses is 13 meV (FWHM). Solid lines: Results of the Monte Carlo simulation. Right-hand side: Transient distribution functions of  $(n = 1)$  electrons (solid lines) as calculated by the ensemble Monte Carlo simulation. Dashed line: Initial Fermi distribution.

the signal vanishes because of carrier cooling on a 50 ps time scale.

In our experiments, the total number of electrons is constant, i.e., excitation and subsequent relaxation processes lead exclusively to carrier redistribution which is monitored via the changes of interband absorption. After the decay of coherent optical polarizations in the sample which occurs typically within the first 100 fs after excitation, the observed absorption change is simply determined by the difference of the transient and the initial equilibrium electron distribution functions [15].

Midinfrared intersubband excitation creates an athermal electron distribution consisting of excited ( $n = 2$ ) carriers and unexcited ( $n = 1$ ) electrons. Our spectrally and temporally resolved data give detailed insight into both parts of this distribution. *In particular, the transient spectra of Fig. 2 reveal the athermal character of the  $(n = 1)$  electrons for a surprisingly long time interval of 2 ps.* Just after excitation [ $t_D = 0.2$  ps, Fig. 2(a)], we observe a transmission decrease from the onset of

( $n = 1$ ) interband absorption up to the Fermi edge of the initially cold distribution [indicated by the arrow in Fig. 2(a)]. The broad range of enhanced absorption demonstrates a monotonous depletion of ( $n = 1$ ) states over the entire range of in-plane  $k$  vectors from the ( $n = 1$ ) band gap up to the initial Fermi level  $E_{F0}$ . This finding is due to the nearly constant energy separation and dipole moment between the ( $n = 1$ ) and ( $n = 2$ ) subbands. The EMC simulation for 0.2 ps (solid lines) gives a constant depletion of the initial Fermi distribution (dashed line) by 15% of the carriers consistent with the excitation conditions.

For the subsequent carrier thermalization, different types of scattering processes have to be considered, namely, electron-electron scattering within the sea of unexcited electrons [16], and relaxation of the photoexcited carriers first via ( $n = 2$ ) to ( $n = 1$ ) intersubband scattering, followed by interaction of the backscattered electrons with the cold plasma and by intraband scattering by optical phonons. The EMC simulation shows that the rate of electron-electron scattering into states below the initial Fermi level  $E_{F0}$  is strongly reduced by the small fraction of unoccupied states to which electrons can be transferred (Pauli blocking), and by screening of the Coulomb interaction. As a result, the carrier depletion between the band gap and  $E_{F0}$  persists for hundreds of femtoseconds, as is directly evident from the data in Fig. 2. Furthermore, the slow redistribution of cold electrons at those early times demonstrates that intersubband electron-electron scattering makes a minor contribution to the thermalization of the cold plasma. It should be mentioned that much faster thermalization of ( $n = 1$ ) electrons was observed after interband excitation of additional electron-hole pairs [3]. In such a case, the excess electrons populate states above the Fermi sea where Pauli blocking and screening are much weaker and—thus—thermalization proceeds within 100 fs.

Intersubband scattering by optical phonon emission transfers the ( $n = 2$ ) carriers to ( $n = 1$ ) states which are about 180 meV above the ( $n = 1$ ) minimum. The density of these energetic ( $n = 1$ ) electrons rises with the IS scattering time  $\tau_{IS} = 1$  ps. Thermalization in the ( $n = 1$ ) subband requires a transfer of such electrons towards the bottom of the band where a quasiequilibrium distribution of *all* electrons is formed. This relaxation involves both emission of optical phonons transferring excess energy to the lattice and Coulomb scattering between high- and low-energy carriers, leading to a heating of the cold electron plasma. The transient interband absorption spectra give detailed information on the different thermalization stages. No bleaching due to accumulation of backscattered carriers in high-lying states is detected at the corresponding probe energies around 1.08 eV (not shown in Fig. 2). We conclude that spreading of the backscattered electrons over a broad energy range occurs much faster than the supply of hot carriers by IS scattering with

$\tau_{IS} = 1$  ps. The inelastic Coulomb scattering between cold and backscattered carriers during this redistribution leads to a transfer of cold electrons to states above the initial Fermi level  $E_{F0}$ , corresponding to the formation of a high-energy tail which includes both formerly cold and excited electrons. In Fig. 2, this is evident from the enhancement of induced absorption below  $E_{F0}$  and the bleaching, i.e., population, above  $E_{F0}$ . Between 0.2 and 1 ps, the very broad high-energy tail results in an amplitude of bleaching much smaller than that of induced absorption. For increasing delay times, this distinctly nonthermal distribution evolves towards a hot Fermi distribution with similar amplitudes for enhanced absorption and bleaching. The spectrum after 2 ps is reproduced by such an equilibrium statistics with a carrier temperature of about 100 K. It is interesting to note that the main energy transfer to the cold plasma occurs at times between 500 fs and 2 ps, due to the delayed supply of energetic carriers from the ( $n = 2$ ) subband.

The relaxation scenario derived from the data is fully confirmed by the EMC simulations. The solid lines on the right-hand side of Fig. 2 represent the calculated transient distributions of ( $n = 1$ ) electrons. The transient spectra derived from those distributions (solid lines on the left-hand side of Fig. 2) are in quantitative agreement with the data. The simulation shows that the overall energy content of the electron distributions is increased by reabsorption of phonons which are emitted by backscattered electrons during intrasubband relaxation and reabsorbed by cold carriers. This nonequilibrium phonon effect leads to reduced cooling in the picosecond regime, as will be discussed in detail elsewhere.

In conclusion, we have studied the relaxation behavior of a pure electron plasma after femtosecond excitation from the ( $n = 1$ ) to the ( $n = 2$ ) conduction subband. An intersubband relaxation time of 1 ps was measured which is determined by emission of longitudinal optical phonons. After intersubband scattering, athermal electron distributions were observed up to delay times of 2 ps. The data were analyzed by ensemble Monte Carlo simulations of the carrier dynamics. The calculations demonstrate that picosecond electron thermalization is due to electron-electron scattering with rates strongly reduced by Pauli blocking and screening and to the picosecond supply of hot electrons from the ( $n = 2$ ) subband.

We gratefully acknowledge support from the Deutsche Forschungsgemeinschaft (SFB 296) and from the European Commission through the ULTRAFast network.

- 
- [1] J.L. Oudar, D. Hulin, A. Migus, A. Antonetti, and F. Alexandre, *Phys. Rev. Lett.* **55**, 2074 (1985).
  - [2] T. Elsaesser, J. Shah, L. Rota, and P. Lugli, *Phys. Rev. Lett.* **66**, 1757 (1991).
  - [3] W.H. Knox, D.S. Chemla, G. Livescu, J.E. Cunningham, and J.E. Henry, *Phys. Rev. Lett.* **61**, 1290 (1988).
  - [4] S. Hunsche, K. Leo, H. Kurz, and K. Köhler, *Phys. Rev. B* **50**, 5791 (1994).
  - [5] J. Faist *et al.*, *Appl. Phys. Lett.* **63**, 1354 (1993).
  - [6] A. Seilmeier, H.J. Hübner, G. Abstreiter, G. Weimann, and W. Schlapp, *Phys. Rev. Lett.* **59**, 1345 (1987).
  - [7] M.C. Tatham, J.F. Ryan, and C.T. Foxon, *Phys. Rev. Lett.* **63**, 1637 (1989).
  - [8] P. Lugli, P. Bordone, E. Molinari, H. Rucker, A.M. De Paula, A.C. Maciel, J.F. Ryan, and M. Shayegan, *Semicond. Sci. Technol.* **7**, B166 (1992).
  - [9] Insook Lee, S.M. Goodnick, M. Gulia, E. Molinari, and P. Lugli, *Phys. Rev. B* **51**, 7046 (1995).
  - [10] J. Faist, F. Capasso, D.L. Sivco, C. Sirtori, A.L. Hutchinson, and A.Y. Cho, *Science* **264**, 553 (1994).
  - [11] F. Seifert, V. Petrov, and M. Woerner, *Opt. Lett.* **19**, 2009 (1994).
  - [12] S.M. Goodnick and P. Lugli, *Phys. Rev. B* **37**, 2578 (1988); S.M. Goodnick and P. Lugli, in *Hot Carriers in Semiconductor Nanostructures*, edited by J. Shah (Academic Press, Boston, 1992), pp. 191–234.
  - [13] A. Tomita, J. Shah, J.E. Cunningham, S.M. Goodnick, P. Lugli, and S.L. Chuang, *Phys. Rev. B* **48**, 5708 (1993).
  - [14] The population of high-lying ( $n = 1$ ) states makes no contribution to the bleaching signal at  $E_{pr} = 1.14$  eV. Because of the different dispersion of the ( $n = 1$ ) and ( $n = 2$ ) valence bands, the interband transitions monitoring such ( $n = 1$ ) populations occur at  $E_{pr} \approx 1.08$  eV.
  - [15] Under such conditions of constant carrier density, many-body effects like changes of the carrier energy renormalization or changes of the Coulomb enhancement of interband absorption play a minor role compared to the population effects [see, e.g., Hailin Wang *et al.*, *Phys. Rev. B* **52**, R17 013 (1995)].
  - [16] Because of the low carrier energy ( $E \leq 18$  meV), emission of optical phonons by the cold carriers can be neglected.